ARTICLE

Surface Functionalization, Oxygen Depth Profiles, and Wetting Behavior of PET Treated with Different Nitrogen Plasmas

Carmen López-Santos,*,† Francisco Yubero,† José Cotrino,†,‡ and Agustín R. González-Elipe†

Instituto de Ciencia de Materiales de Sevilla, CSIC-Universidad de Sevilla, Avenida Américo Vespucio 49, 41092 Sevilla, Spain, and Física Teórica, Departamento de Física Atómica, Molecular y Nuclear, Facultad de Física, Universidad de Sevilla, Avenida Reina Mercedes, 41012 Sevilla, Spain

ABSTRACT Polyethylene terephthalate (PET) plates have been exposed to different nitrogen containing plasmas with the purpose of incorporating nitrogen functional groups on its surface. Results with a dielectric barrier discharge (DBD) at atmospheric pressure and a microwave discharge (MW) at reduced pressure and those using an atom source working under ultrahigh vacuum conditions have been compared for N_2 and mixtures Ar + NH_3 as plasma gases. The functional groups have been monitored by X-ray Photoemission Spectroscopy (XPS). Nondestructive oxygen and carbon depth profiles for the plasma treated and one month aged samples have been determined by means of the nondestructive Tougaard's method of XPS background analysis. The surface topography of the treated samples has been examined by Atomic Force Microscopy (AFM), while the surface tension has been determined by measuring the static contact angles of water and iodomethane. It has been found that the DBD with a mixture of Ar+NH_3 is the most efficient treatment for nitrogen and amine group functionalization as determined by derivatization by reaction with chlorobenzaldehyde. It is also realized that the nitrogen functional groups do not contribute significantly to the observed increase in surface tension of plasma treated PET.

KEYWORDS: surface treatment • nitrogen plasma • ammonia groups • wetting angle • PET • depth profile

1. INTRODUCTION

Surface functionalization of polymers and related materials by plasma techniques is a current technology of surface activation. Control of wetting contact angle, development of bioactive or biocide surfaces, or improvement of adhesion are some of the fields of application of the plasma technologies (1−6). In general, the plasma treatments aim at the incorporation of functional groups such as −OH, $-NH_2$, −COOH, etc., on the surface of the treated materials. In this context, plasmas of nitrogen or ammonia, either pure or mixed with noble gases, have been proposed for the incorporation of nitrogen functional groups on the surface of polymeric materials (7−12). These plasmas have been excited with microwave, radiofrequency, or more recently, other procedures at atmospheric pressure (11, 12). Other alternatives for the surface incorporation of nitrogen functional groups is the plasma copolymerization of insaturated hydrocarbons with N_2 or NH_3 (13, 14) or by direct polymerization of allylamine, either with low- or atmospheric pressure plasmas (15, 16). N-rich surfaces have been found to promote cell adhesion and be effective for the covalent coupling with proteins and signal molecules (13, 17−19).

In the present work, we have carried out a systematic study of the plasma functionalization of PET to incorporate nitrogen functional groups, particularly amino groups, onto its surface. Nitrogen functionalization of PET by means of plasma has been intended previously by other groups (20, 21). A first purpose of the present work is to determine the main factors favoring the surface functionalization of this polymer and to understand the effect of the different process parameters on its surface modification. In particular, a critical point with an oxygenated polymer like PET is to assess not only the effectiveness for the incorporation of nitrogen functional groups but also to determine the changes induced in the chemical nature and in the depth distribution of nitrogen, oxygen, and carbon in the first surface layers of the treated polymers. A related problem is to assess to what extent these changes or the characteristics of the nitrogen surface groups induced by the plasma are responsible for the modification of the surface tension of the plasma-treated polymers. The problem of whether nitrogen functional groups, in particular amino groups, are able to induce changes in the surface hydrophilicity is controversial and contradictory results have been published on this subject (20−24). Another related issue is the study of the stability of amine groups formed on the surface of functionalized PET and their evolution with time (i.e., aging). This point has also deserved the attention of several authors who, on different surface activated polymers, have studied the factors contributing to the removal of amine groups from the surface (25, 26).

To get a deep insight into these questions and their dependences on the plasma characteristics, we have carried out a systematic study by using three different methods of

* Corresponding author.
Received for review August 17, 2009 and accepted March 1, 2010
† CSIC-Universidad de Sevilla.
‡ Facultad de Física, Universidad de Sevilla.
DOI: 10.1021/am100052w

Published on Web 03/10/2010

surface activation. These procedures include low-pressure MW plasma, atmospheric pressure DBD plasma, and a beam of neutral species containing nitrogen. In comparison with MW plasmas, DBD discharges present a filamentary component (27) and a higher concentration of activated neutral species (28). Meanwhile, the effect of a neutral beam of nitrogen species on PET under quite well controlled vacuum conditions provides a reference system to compare the effects produced by the more conventional plasma treatments based on MW or DBD discharges.

As analysis tools, we have used X-ray photoemission spectroscopy (XPS), water and iodomethane contact angle (WCA) measurements for estimation of the surface tension (29, 30), and atomic force microscopy (AFM) for the characterization of the surface topography, just after the plasma treatments or after storage for 1 month. A very important issue is the assessment of the in-depth oxygen and carbon distributions after different plasma treatments. With this aim, we have used the XPS peak shape analysis developed by Tougaard (31, 32). This analysis provides a semiquantitative description of the oxygen/carbon in depth distributions for both the "as-treated" and "aged" polymers. To the best of our knowledge, this method has not been used before to characterize polymers except in a previous work by us where we determined the oxygen in-depth distribution in PET and PE (i.e., polyethylene) exposed to different oxygen plasmas (33). A related aspect of the present investigation is the study of the time evolution of the depth profiles of the treated PET. Aging is a common process in polymeric materials subjected to oxygen plasma activation (1, 2, 7) but less is known about similar processes in PET treated with nitrogen plasmas, particularly if we refer to the possible evolution of the composition depth profiles of the outmost surface layers. A final methodological issue is the determination of the relative amount of amino groups formed on the surface of the treated PET. Determination of amino groups can be carried out by reaction with a labeling compound and posterior analysis by XPS (34−36). Here, we have used the derivatization method proposed by Chevallier et al. (36) consisting of the reaction of amino groups with chlorobenzaldehyde. The results obtained reveals that the amount and type of nitrogen species at the surface are quite dependent on the type of plasma procedure used for activation.

2. EXPERIMENTAL SECTION

Materials. Commercial plates of PET (0.5 mm thickness) were supplied by GOODFELLOW (Goodfellow Ltd., Cambridge). A full account of properties of this material is available by the provider. The plates were subjected to a gentle cleaning with ethanol to remove possible contamination from their surface. These samples will be considered as the "original" samples through all this paper.

Plasma Treatments. Treatments by low-pressure MW plasmas were carried out in a reactor consisting of a quartz tube with a funnel shape termination attached to a stainless steel chamber were the samples were placed. The reactor has a remote configuration and the samples were exposed downstream to the plasmas species generated in the quartz tube by a surfatron (37) launcher that was supplied with a microwave power of 60 W. A scheme of the apparatus can be found in ref 38. A typical density of ionic species of about 1×10^{11} cm^{-3} can be reached with this reacto r (39). The plasma gas consisted of N_2 (17 sscm) or mixtures Ar + NH_3 with Ar as majority component (40 sscm) and NH_3 (1.2 sscm) as minority component. A typical working pressure of 0.3 Torr was used for the experiments. A base pressure of 1×10^{-3} Torr was routinely reached in this reactor. Before igniting the plasma, N_2 or the mixture Ar + NH_3 was kept flowing for at least 30 min to ensure the purity of the plasma gas within the reactor. Exposure times of 1 min were used for these experiments. This time was enough to achieve steady-state conditions for surface nitridation of PET.

The DBD reactor consisted of two active electrodes made of stainless steel. The PET plates to be treated were placed on the bottom electrode acting as a dielectric barrier. The rear part of the polymer was contacted with the metal piece by means of a conductive silver paste. The distance between the upper metallic electrode and the polymer was 1 mm. The discharge between the metal and the polymer surface was induced by an AC high voltage power supply working at a typical voltage of 8 kV and a frequency of 1.5 kHz. Under these conditions, formation of small filaments was evidenced by means of an oscilloscope connected in parallel between the two electrodes (33). N_2 (47 sscm) or mixtures of Ar (76 sscm) and NH_3 (2 sscm) were used for these treatments. Before the plasma was ignited, a continuous flow of the gas mixture was maintained through the reactor to ensure that no traces of air remain in the reaction chamber. This was checked by mass spectrometry analysis of the outlet gases. Typical treatment times of 1 min were used by this procedure. In this system, the density of ionic species reaches a value of 1×10^9 cm^{-3}, approximately (40).

After the samples were subjected to the different treatments, they were stored in air at room temperature in a diseccator until their analysis by XPS or the contact angle measurements.

Treatments with Neutral Species. These experiments were carried out "in situ" in the same XPS apparatus used for the analysis of the samples treated by DBD and MW plasmas. The samples were exposed in the pretreatment chamber to a beam of neutral atoms/species generated with an Oxford OSPrey source (Oxford, UK) supplied with pure nitrogen or ammonia at a pressure of 5×10^{-5} Torr. The base pressure in this pretreatment chamber was 2×10^{-8} Torr. In comparison with the two other plasma treatments, it is important to stress that the presence of oxygen species in the beam must be extremely low and its effect on the surface of the polymer practically negligible (e.g., by assuming that all the base pressure of the chamber is due to water, a first approximation would yield a ratio of 2500:1 for the ratio of nitrogen to oxygen species). The source is an ECR MW system with an extraction grid. If that extraction source is switched off, the system produces a beam of thermalized atoms or neutral species (i.e., with a kinetic energy smaller than 1 eV according to the supplier information). In comparison with the MW and DBD plasmas, we will assume that neutral, nonaccelerated species are impinging on the surface of the polymer. A way of estimating the dose of species arriving to the substrate is to measure the beam current on the substrate when selecting the ion option as an operating mode of the source. This measurement yielded an approximate value of 0.1 μA cm^{-2}. Taking this value into account and the information of the supplier about the dissociation degree of nitrogen it is possible to make a rough estimation of the number of neutral species arriving to the surface of the sample. A calculated value of 5×10^{13} atoms cm^{-2} s^{-1} has been obtained for the sample situated 10 cm apart from the source. This flow of neutral species ensures that a steady state has been obtained for the sample surface after the exposure times used in this experiment. A similar calculation was not possible when the source was supplied with ammonia. In this case, hydrogen, nitrogen, and NH_x neutral species (in the text we will denote this situation as N−H_x) are

impinging on the surface of the polymer. These species were detected by a mass spectrometer placed at the sample position.

XPS spectra were taken after ensuring that the sample composition (i.e., N/C/O ratios) had reached a steady state. Because the beam density provided by this source was relatively small, long exposure times of up to 30 min were used in most experiments. Thus, this exposure time was used to get the spectra presented in the manuscript. Experiments were also carried out for shorter and longer times to assess the effectiveness for nitrogen incorporation under these experimental conditions. The obtained results are included in the Supporting Information. The samples treated for 30 min were also investigated by AFM and wetting angle measurements after they were taken out from the XPS apparatus.

Analysis Methods. The surface tension and wetting properties of PET were determined by measuring the wetting contact angles (WCA) of water and iodomethane (29, 30). The roughness was determined by AFM and the chemical and in-depth composition by XPS before and after the polymer was subjected to the different treatments. WCA measurements were taken for the samples immediately (within few minutes) after the MW and DBD plasma treatments or after the analysis by XPS of the samples treated with the neutral beams.

Regarding the XPS characterization, a time comprising between 30 and 60 min was needed to introduce the samples in the XPS apparatus after the plasma treatments. XPS spectra were acquired 6−8 h afterward (time needed to achieve the minimum vacuum conditions required for perform measurements). Besides these studies with the freshly treated samples, other analyses were carried out with the samples kept in a diseccator for different periods of time. Thus, XPS and WCA measurements were done after 1 day, 1 week, and 1 month storage.

XPS spectra at normal takeoff angles were recorded with a PHOIBOS-100 5MCD (SPECS) electron spectrometer working in the constant pass energy mode fixed at a value of 20 eV. An unmonochromatized Mg Kα radiation was used as excitation source which, in part, was responsible for a relatively low resolution of the spectra. Pressure during acquisition was about 5×10^{-9} mbar. For calibration of the binding energy (BE) scale, a value of 284.5 eV was assigned to the C 1s component attributed to C−H and C−C bonds. Average surface composition was estimated by calculating the area behind the C1s, O1s, and N1s peaks and by correcting the obtained values with the corresponding sensitivity factors. Because of the fact that the signal of carbon atoms attached to nitrogen functional groups appears in the same region as that of carbon bonded to oxygen groups (41−43),no fitting analysis of the C1s signal has been intended. Similarly, no quantitative evaluation of the type of surface functional groups was intended by fitting analysis of the O1s or N1s peaks.

Evaluation of the amount of amino groups on the surface of the treated samples was done by vapor phase chemical derivatization following the method of Chevallier et al. (36). This method consists of letting the sample for a minimum period of three hours in contact with the vapors of chlorobenzaldehyde (Aldrich, Spain) heated at 55 °C. This reaction period was sufficient to get steady state conditions as no further reaction could be detected after 2 h of contact. According to these authors, after this period, the following specific reaction involving amino groups takes place at the surface:

$$Cl{-}C_6H_4{-}CHO + NH_2{-}[R] \rightarrow Cl{-}C_6H_4{-}CH{=}N{-}[R] + H_2O \quad (1)$$

This reaction implies the surface incorporation of one chlorine atom and seven new carbon atoms per amino group. After the reaction has taken place, the specimens were brought to the spectrometer where the atomic concentration of chlorine atoms anchored on the surface was measured. In this regard, it was very carefully checked that no losses of chlorine occurs during the analysis by XPS as a result of the X-ray irradiation in vacuum. This concentration can be correlated with the amount of amino groups reacted according to formula 1. An estimation of the concentration of nitrogen atoms in the form of amino groups can be done according to the formula (44)

$$[NH_2] = [Cl]/([C] - 7[Cl]) \quad (2)$$

where $[NH_2]$ is the concentration of nitrogen in the form of amino groups. Meanwhile, [Cl] and [C] are, respectively, the concentrations of chlorine and carbon atoms detected on the plasma-treated surfaces after the derivatization process. The error bar for the determination of the amine concentration has been estimated in ±0.2%.

The in-depth distribution of C and O atoms within the surface region (up to 6−10 nm depth) of the samples before and after plasma treatments was assessed by XPS peak shape analysis using the QUASES software (45). The XPS peak shape analysis method relies on the fact that the inelastic background that appears in the low kinetic energy side of a photoelectron peak carries information on the depth of origin of the detected electrons (34, 35, 45). Thus, wide scan spectra of C1s and O1s peaks (i.e., including their inelastic background) were analyzed according to this procedure. Clear changes in the in-depth distribution of the C and O atoms were found after the different activation treatments and aging periods. A similar analysis was also intended with the nitrogen signal. However, because of the relatively low intensity of this signal no reliable data could be obtained in this case and the results will not be considered here. For comparison, angle-resolved analysis was also carried out to confirm the tendencies in depth distribution found by using the background analysis method. Spectra were recorded at 90, 70, and 45° take off angles (see the Supporting Information).

Static WCA measurements were carried out by the Young method by measuring the contact angle of small water and iodomethane droplets (5 μL) with a CAM100 instrument (KSV Instruments Ltd., Finland). Carefully deionized and bidistilled water was used for these experiments. The reported values are an average of a minimum of seven measurements taken for each examined surface. Although a straightforward analysis of the surface tension of plasma treated polymers requires the measurement of both the advancing and receding wetting angles (46), in the present work we just present static contact angles because our purpose is the comparative assessment of the effects of three different methods of surface activation. In a similar way, contact angles of iodomethane were measured to determine the polar and nonpolar contributions to the surface tension by the Owens−Wendt−Kaelble approximation (47).

Topographic images of the surface were taken with a Nanotec AFM microscope and a Dulcinea electronics, working in tapping mode and using high frequency levers. AFM images were processed with the WSxM software. For each polymer, more than five good-quality images were taken at different regions of the sample after the different treatments. The derived rms values were determined for a representative image of the surface and agree well with the average values of all images.

3. RESULTS

Standard XPS Analysis of Functional Groups after Plasma and Beam Treatments. XPS has been used to assess the chemical changes that occur at the PET surface exposed to the different plasmas and/or neutral beams. Figures 1−3 show the C1s, O1s, and N1s spectra of

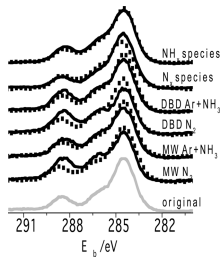

FIGURE 1. C1s photoemission spectra of PET subjected to the indicated surface activation treatments by plasma and a beam of neutral species (black lines) and for these films after storage for 1 month (dotted lines).

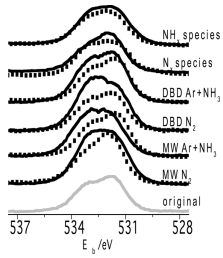

FIGURE 2. O1s photoemission spectra of PET subjected to the indicated surface activation treatments by plasma and a beam of neutral species (black lines) and for these films after storage for one month (dotted lines).

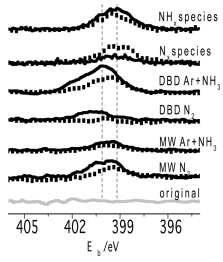

FIGURE 3. N1s photoemission spectra of PET subjected to the indicated surface activation treatments by plasma and a beam of neutral species (black lines) and for these films after storage for 1 month (dotted lines). The dashed lines are plotted to guide the eyes.

Table 1. Atomic Percentages in PET Subjected to the Indicated Treatments[a]

sample/ treatment	C % (1 h)	O % (1 h)	N % (1 h)	C % (1 month)	O % (1 month)	N % (1 month)
PET original	74.2	25.8	0			
MW Ar + NH_3	64.0	34.7	1.3(0.7)	67.5	31.3	1.2(0.1)
DBD Ar + NH_3	62.8	33.1	4.1(0.8)	67.2	30.5	2.3(0.5)
N−H_x species	70.0	26.3	3.7(0.3)	71.0	26.4	2.6(0.3)
MW N_2	62.7	35.3	2.0(0.4)	65.4	32.6	2.0(0.0)
DBD N_2	58.9	40.4	0.7(0.2)	69.5	30.4	0.1(0.0)
N species	71.0	26.5	2.5(0.3)	70.9	27.9	1.2(0.0)

[a] In parentheses, percentage of chlorine determined after derivatization according to ref 36.

samples just after their treatment and after their storage for one month. Meanwhile, Table 1 reports, expressed in the form of atomic percents, the surface composition determined with this technique for PET subjected to the different plasma and beam treatments. This table shows that the percentage of nitrogen is higher for the DBD/(Ar + NH_3) plasmas. In comparison, DBD/N_2, MW/N_2, and MW/(Ar + NH_3) plasmas are less efficient for the incorporation of nitrogen. In fact, the atomic percentage of nitrogen reaches a value of 4% for the DBD/(Ar + NH_3) plasma and only 2% for the MW/N_2 plasma. Meanwhile, the oxygen content increases to 33, 35, and 40% for the DBD/(Ar + NH_3), MW/(Ar + NH_3) or MW/N_2, and DBD/N_2 plasmas, respectively. It is apparent from this evolution that the presence of some oxygen species in the nitrogen plasmas, likely coming from the residual impurities of oxygen and/or water in the chamber, may lead to a decrease in the effectiveness for the surface functionalization with nitrogen. It is important to note that plasmas with NH_3 are more effective for this aim so that although the oxygen on the surface content increases, the incorporation of new nitrogen functional groups is also more effective. The treatment of PET with neutral species coming from the atom source produces slightly different results. Thus, almost no increase in the concentration of oxygen species is found after the treatment with the neutral N or N−H_x beams. By contrast, the concentration of nitrogen onto the surface reaches in the two cases values of the order of 3−4%, close to the maximum concentration of nitrogen found after treatment with the DBD/(Ar + NH_3) plasmas.

The C1s spectra of the original PET is characterized by a series of peaks and shoulders that, for the original samples, have been previously attributed in literature to different surface groups: −COH/−C−O−C− (BE at 286.0 eV), −CO (BE at 287.5 eV) and −COOH/−COOR (BE at 288.6 eV) (20−22, 48, 49). The relative intensity of these peaks and shoulders is slightly modified after the different plasma treatments. This implies a change in the partition of these surface groups and/or the contribution of new functionalities involving nitrogen species. Because of the superposition in this spectral region of the components of the functional groups of carbon species bonded to oxygen and/or nitrogen, no fitting analysis will be intended here.

In parallel, changes occur at the O1s signal. The spectrum and the oxygen atomic concentration of the original sample fits well with the actual composition of this polymer (i.e., 28% atomic) and with previously reported data by XPS for this material (20−22, 48, 49). The spectrum of the original PET is characterized by two contributions at 531.7 and 533.2 eV, generally attributed to, respectively, the presence of surface groups of carboxy type (i.e, oxygen double-bonded to carbon in acetone, aldehide or carboxyl groups, band A at 531.7 eV) and ether or alcohol type (i.e., oxygen single-bonded to carbon in ether or hydroxyl groups, band B at 533.2 eV) (50). After the different nitrogen plasma treatments, we found a significant increase in the oxygen concentration at the surface (cf. Table 1). Simultaneously, the shape of the spectra underwent a change with respect to that of the original material that was characterized by a relative increase in the intensity of the component B at 533.2 eV. Aging for 1 month restored both the shape of the spectra and, partially, the relative O/C ratio of the original material (cf. Table 1 and Figure 1). A possibility to account for these changes is that some oxygen impurities excited by the plasma react with the surface of the polymer leading to the preferential formation of species B. This possibility has been

previously proposed by us to account for similar effects during the plasma functionalization of DLC (diamond like carbon) by the same type of nitrogen plasmas (51). The reaction of minority oxygen species present in the nitrogen plasmas with the surface of polymers has been also referred previously in the literature (52). However, the fact that a similar change in the A/B ratio also occurs when the polymer sample was exposed to the neutral species of N or $N-H_x$ under a virtual complete absence of oxygen in the environment (Figure 2, bottom) might also sustain that nitrogen species preferentially reacts with the oxygen functional groups of type A.

Figure 3 and Table 1 also show that nitrogen becomes incorporated onto the PET sample when this material is exposed to the plasmas and/or to the beams of neutral species. Nitrogen incorporation is characterized by the development of a XPS signal with a BE between 399 and 402 eV. This result points to the formation of functional groups of the type $C-NH_2$, C═N, and/or C−N (7−9, 43, 52). The fact that the width of the spectra lies in all cases between 2.4 and 2.5 eV (the main C1s fitting band at 284.5 eV has a width of 1.6 eV) suggests that the recorded spectra are the result of the contribution of several types of functional groups. However, a direct identification of the different nitrogen species formed in each case is not straightforward due to the slight difference in BEs of the aforementioned functional groups and the absence of well-defined shoulders/bands in the experimental spectra. For a similar situation with functionalized polymers, Gerenser et al. (7, 8) suggested that a qualitative assessment of the functional groups is possible by following the evolution of the centroid of the experimental band. Bands close to a BE of 399.2 eV would suggest the formation of amine-like species, whereas a band shifted to higher BE would indicate the formation of imide, amide, and other nitrogen species. The N1s spectra in Figure 3 evidence a certain shift toward 399.2 eV in the position of the peaks for the DBD/(Ar + NH_3) and the neutral beam treated samples (see the two lines plotted in the figure to guide the eyes). It is thus likely that the concentration of amine groups is higher in these samples and that, in general, it may change according to the procedure used to activate the surface. However, because other nitrogen groups besides amine can be also formed on the surface of the treated PET, shifts in the centroid of the N1s spectrum cannot be taken as an absolute evidence of the formation of this type of functional groups.

For the samples stored for one month after the treatment, the surface concentration of oxygen decreases significantly. A similar decrease, particularly intense for the DBD treated samples, is found for the nitrogen concentration that may almost disappear from the surface in some cases (e.g., for samples treated with the DBD/N_2 plasmas).

Assessment of the Formation of Amino Groups by Surface Derivatization. To further characterize the type of nitrogen species formed at the surface and, in particular, to assess the incorporation of amino surface groups, we have exposed the plasma treated PET to vapors of chlorobenzaldehyde following the protocol described in the experimental section. According to Chevallier et al. (36) the process taking place during this experiment can be described according to reaction 1, so that the surface concentration of chlorine after reaction can be related with the surface concentration of amino groups before reaction. We also carried out control experiments on untreated PET and found a negative result (i.e., no chlorine appeared onto this surface). Cl2p photoemission spectra were simultaneously recorded (see the Supporting Information). The amount of chlorine anchored onto the surface in previous experiments with other materials making use of similar derivatization treatments was in the order of magnitude of the quantities detected in our case (36).

As a general result, it is found that the surface concentration of nitrogen atoms decreases and that of carbon increases after derivatization. According to reaction 1, these results agree with that per each reacted amino group seven carbon atoms and one chlorine atom of the chlorobenzaldehyde radical are incorporated onto the surface. Some additional contamination of the surface of samples during their handling in air and the treatment with the chlorobenzaldehyde vapors might also contribute to this finding.

The percentages of chlorine atoms reported in parentheses in Table 1 indicate that the DBD/(Ar + NH_3) plasma treatment produces the maximum concentration of $-NH_2$ surface groups followed by the MW/(Ar + NH_3) treatment. It also appears that the DBD/N_2 plasma is less effective in generating amino groups with a surface concentration of 0.2% of Cl atoms detected in the derivatized sample. In the two samples exposed to the nitrogen beams, only a small concentration of chlorine atoms (i.e., 0.3%) was found despite the relatively high concentration of incorporated nitrogen. It is important to mention that, in general, the percentages of nitrogen and to a lesser extent oxygen decrease after derivatization. This result must be related with the aforementioned shadowing effect produced by the anchored chlorobenzaldehyde radicals and/or with the occurrence of side reactions leading to the removal of functional groups. Because in our experiments the incorporation of chlorine atoms is always much smaller that the amount of removed nitrogen, it is also likely that some chlorine may be lost in the reaction medium. Side reactions leading to the loss of the atoms used as a probe have been claimed for polymer surfaces containing nitrogen that were derivatized by reaction with 4-trifluormethylbenzaldehyde (53). Therefore, we think that our derivatization data should be considered as semiquantitative and usable for comparative purposes only. On this basis, we have calculated the surface concentration of nitrogen in the form of amino groups for the samples just after their activation and aged for one month. These concentrations are shown in Figure 4. In comparison with the total nitrogen concentration on the surface, it is apparent that only a portion is in the form of amines. As stated above by the assessment of the chlorine concentrations (c.f., Table 1), maximum concentration of amino group occurs for the DBD/Ar+NH_3 and MW/Ar+NH_3

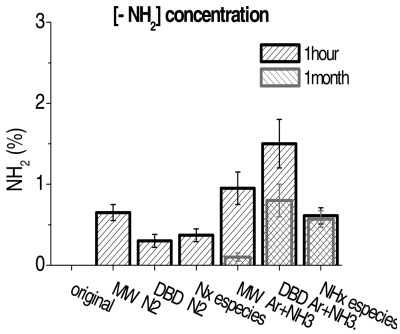

FIGURE 4. Concentration of nitrogen in the form of amino groups for the PET subjected to the indicated activation treatments and for these samples after their aging for 1 month.

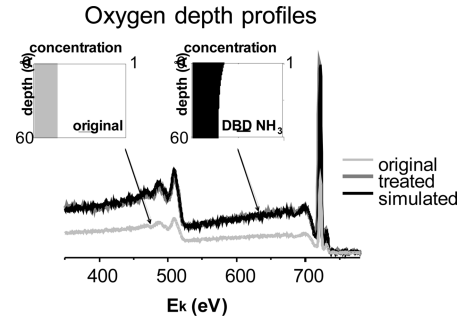

FIGURE 5. O1s wide scan spectra of the original PET and of this sample treated with the DBD/(Ar + NH_3) plasma. The simulated spectrum that best fits this latter is also included in the figure (black line). The two insets show the oxygen depth profiles determined from background analysis of the spectra of the original and plasma-treated sample.

plasmas. It is also important to note in this figure that after the aging period, amine groups remain only on the surface of these two samples and on that treated with the N−H_x species.

Oxygen and Carbon In-Depth Distributions from XPS Peak Shape Analysis. Analysis of atomic in-depth concentration profiles by XPS peak shape analysis according to the Tougaard's concepts can be used to estimate the depth distribution of a given atom in a solid sample (31, 32). To the best of our knowledge, this technique has been only used with polymers in a previous work of us where we studied oxygen depth profiles in PET and polyethylene exposed to different plasmas of oxygen (33). Previous studies in literature by other techniques have estimated that oxygen can penetrate up to several nanometers of the outmost surface layers after oxygen plasma activation (27). Trying to get a closer look to the element in-depth distribution in PET, we have applied XPS peak shape analysis to the oxygen and carbon photoemission signals in the fresh plasma treated polymer and for these treated samples after aging for one month. It is important to remark that although we also tried to apply this method to determine nitrogen depth profiles, the small intensity of the N 1s signal and the absence of significant differences in the backgrounds behind the N1s peak precluded the use of this technique to assess distribution profiles of this element.

The basic principle of the method relies on describing properly the inelastic losses induced by electron transport through a given material. It is assumed that, after excitation by the X-rays, the primary spectrum $F(E)$ transforms into the actually measured spectrum $J(E)$ because of the energy losses undergone by the primary electrons during their transport through the analyzed material. For the analysis carried out here, it is assumed that the $F(E)$ functions for carbon and oxygen in the original PET correspond to a homogeneous in-depth distribution of these elements and that the probability for energy losses due to electron transport is governed by the polymer-type inelastic scattering cross sections included in the QUASES software package (45).

The in-depth distributions of oxygen and carbon atoms after the different activation procedures and aging periods were estimated by a trial and error method where several parameters describing the in-depth profile (surface coverage, bulk coverage, and characteristic length in an exponential distribution) were varied until a good agreement between simulated and measured spectra is achieved.

As an example of the differences in the shape of the backgrounds and the derived depth profiles, Figure 5 shows wide scan spectra corresponding to the O1s signal of PET before and after being exposed to the DBD/Ar + NH_3 plasma. The spectra have been normalized to the intensity of the elastic O 1s peak to stress the relative changes in the inelastic backgrounds. The figure also shows the simulated spectrum of the plasma-treated PET and the depth profiles determined with the QUASES software for the original and plasma treated samples. It is apparent in this figure that through the whole spectral range the background of the plasma-treated PET presents a higher intensity than the original polymer and that this background can be reproduced accurately by the theoretical analysis. In comparison with the oxygen depth profile of the original PET taken as flat for the analysis, the oxygen distribution after plasma treatment evidence an enrichment of oxygen at the surface and an overall increase in oxygen concentration, at least through the depth proven by the background analysis (i.e., approximately 6−10 nm).

By a systematic analysis of the XPS photoelectron peak shape with the help of the QUASES software we have obtained carbon and oxygen depth profiles for all the studied samples. A representation of these profiles is shown in Figure 6 for PET subjected to the different treatments and for these samples after storage for one month. For PET subjected to both DBD and MW plasmas, the profiles confirm an enrichment of oxygen in the topmost surface layers (i.e., in the 2−3 topmost nanometers). This enrichment is different depending on the actual treatment and is accompanied by a decrease in the relative concentration of carbon from these surface layers. By contrast, the oxygen and carbon depth profiles of PET exposed to the beams of neutral species depict a different behavior. Thus, while the carbon profile is almost flat through the entire depth, the oxygen concentration decreases at the surface for PET exposed to the N species and remains almost flat for PET exposed to the N−H_x species. It is worthy of note that these results are not contradictory with the quantitative analysis of the oxygen content in the samples reported in Table 1, because the values in this table are averaged percentages

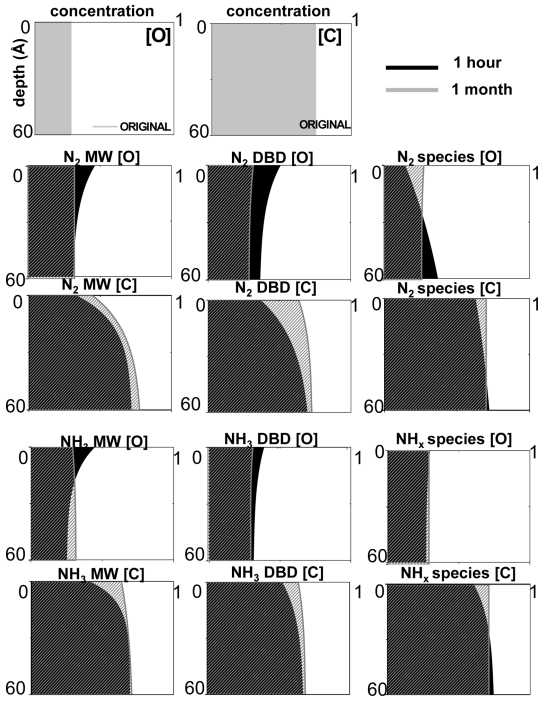

FIGURE 6. Calculated depth profiles of oxygen and carbon for PET subjected to the different plasma and beam treatments. Continuous full gray and black color profiles correspond to the original and plasma and beam treated samples, respectively, whereas the dashed profiles correspond to the samples aged for 1 month.

corresponding to the whole sample thickness from which the elastic photoelectrons are ejected (the estimated mean free path of the O1s electrons in polymers is of about 23 Å (54)). It can be proposed as a reasonable hypothesis that the oxygen depletion from the surface is related with the need of a critical time to induce the formation of nitrogen species on the surface (see the Supporting Information). This result suggests that the first nitrogen atoms arriving to the surface react with the oxygen groups forming volatile molecules and only when the oxygen surface concentration decreases nitrogen functional groups become bonded to the surface.

The traditional method to nondestructively estimate composition depth profiles in polymers is by recording XPS spectra of the same sample at different takeoff angles. To validate the results obtained by the background analysis procedure, we have also carried out this type of measurement and found the same tendencies for the oxygen enrichment at the surface revealed by the background analysis method. Selected results of angle-resolved experiments are presented in the Supporting Information.

It is also important to note in Figure 6 that although oxygen and carbon present complementary profiles, they do not necessarily sum to 100% because of the presence of nitrogen in the outmost surface layers of the treated samples (cf. Table 1). When the samples are stored for one month, the concentration profiles changed, approaching the flat profiles of the original PET. Similarly to the case of PET exposed to the different plasmas, the profiles in Figure 6 for the beam-treated polymer recover their original shape after aging for one month.

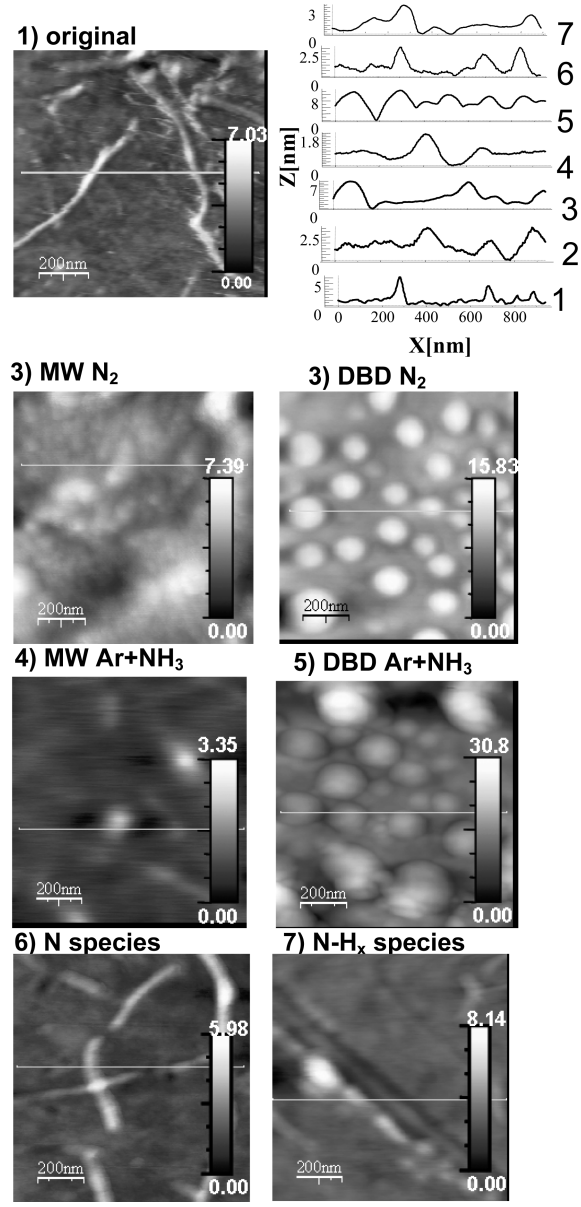

FIGURE 7. AFM images of the PET surface subjected to the indicated treatments. Line profiles according to the straights drawn in the images are included in the top-right plot. Contrast scale units: nanometers.

Surface Topography of Plasma-Treated PET. Plasma treatments of polymers induce not only a chemical functionalization of their surface but also a change in their surface topography. To assess these changes, we have carried out an AFM analysis of the plasma treated samples.

Figure 7 shows images corresponding to PET before and after being subjected to the different surface activation treatments. In addition to the images, the figure also shows line profiles taken along the straights plotted in the reported images. The different surface topographies found and the different color scales of the images clearly support the existence of significant differences in roughness depending on the plasma treatments The rms values summarized in Table 2 confirm these differences.

For the original PET, a general observation is the existence on its surface of a kind of fiberlike structure. A similar

Table 2. RMS Values of PET Subjected to the Indicated Treatments

sample/treatment	rms /nm(1 μmx1 μm)
PET original	0.8
MW Ar + NH_3	0.3
DBD Ar + NH_3	4.2
N−H_x species	0.7
MW N_2	1.0
DBD N_2	1.8
N species	0.7

topography has been reported in other studies (55). The image contrast of this kind of fibres is enhanced as a result of the MW plasma treatments. It can be also assessed from the line profiles in Figure 7 and the rms values in Table 2 that this polymer is rather flat and that the rms values slightly decrease after the MW and beam treatments. The two DBD plasmas, particularly the DBD/(Ar + NH_3) one, produce an increase in roughness and the formation of small agglomerates on the surface that substitute the fiberlike topography of the original material. A similar topography for this polymer treated with a DBD plasma of oxygen was reported by Strobel et al. (46), who attributed the grainlike surface features to the agglomeration of low molecular weight fragments produced by the oxidation of the long chains of the amorphous component of the polymer. In a previous publication, we reported a similar behavior for PET exposed to DBD/O_2 plasmas (33).

Surface Energy of Plasma- and Beam-Treated PET. Figure 8 shows the changes in the static water contact angles for the PET surfaces treated with the different plasmas/beams, as well as the evolution of these magnitudes with aging time. Water wetting angles significantly decreased after the plasma treatments with changes higher than 45 % in this parameter. It is also important to remark that the wetting angle recovers partially with the aging time, except for the DBD/N_2 plasma where this parameter is still 20 % smaller than in the original sample. This figure also shows that the decrease in wetting angle for PET subjected to the beam treatments is quite small (only changes of 17 and 7 % for the N−H_x and N beam treatments, respectively) and that it completely recovers the original value after storage for 1 week.

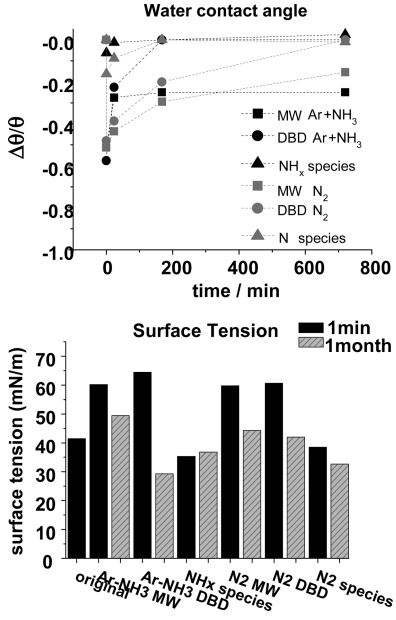

FIGURE 8. (Top) Water contact angle of PET subjected to the indicated plasma and beam treatments and then aged for the indicated period of time. (Bottom) Surface tension of PET just after its surface activation by plasma and beam treatments and after storage for 1 month.

Figure 8 also shows the surface tension values determined according to the method of Owens−Wendt−Kaelble (47) from the contact angle data of water and iodomethane. Although the reported values must be only considered for comparative purposes (determination of real surface tension values would require the use of at least three different liquids) they show that the surface tension increases after the different plasma treatments (roughly from about 40 mN m^{-1} for the original sample to a value around 60 mN m^{-1}), but undergo very little changes or even decreases for PET exposed to the beam treatments. In all cases, after 1 month, the surface tension approaches the value of the original PET.

4. DISCUSSION

The previous results on PET have provided valuable information about current, not yet understood, questions related with the nitrogen plasma activation of polymers and the characteristics and stability of the amine groups formed onto their surface (25, 26). Namely, we have gained a deeper insight into the following questions:

(a) Dependence of the effectiveness of nitrogen functionalization of PET on the type of plasma and plasma gas

(b) The hydrophilic character of the amine groups and the influence of aging in the stability and wetting properties of plasma functionalized PET

(c) The depth distribution profile of oxygen and nitrogen species in plasma treated polymers.

Plasma Characteristics and Effectiveness for Nitrogen Surface Functionalization of PET. The previous results have shown that the treatment of PET with a series of nitrogen plasmas/beams induces the incorporation of nitrogen functional groups onto its surface. Our results have also shown that nitrogen incorporation effectiveness is highly dependent on the type of plasma, following the order: DBD/Ar + NH_3 > MW/Ar + NH_3 > MW/N_2 > DBD/N_2. A high effectiveness for nitrogen incorporation is also found for the neutral beams of nitrogen (N and N−H_x) species. A significant difference between DBD atmospheric plasma and low pressure MW plasma is that, in the former case, neutral active species are more abundant than in the latter. The opposite happens with regard to the concentration of ionized species (56−58). Therefore, these results suggest that neutral species are more active for nitrogen surface functionalization of PET. The quite significant changes in surface topography found after these treatments (see Figure 7) also support the high etching activity of the DBD plasmas interacting with PET (33, 46). The effectiveness of neutral species of nitrogen for the surface functionalization

of polymers is further supported by our experimental results with the beams of neutral species. These working conditions provide a beam of very reactive N atoms or NH_x neutral species with no ions or other features like UV photons, quite abundant in conventional plasmas. These neutral beams have promoted the surface incorporation of a substantial concentration of nitrogen functional groups without any significant increase in the oxygen content at the surface.

For the DBD plasmas, it is also found that ammonia mixed with Ar is more effective than nitrogen as plasma gas. Previous characterization studies by optical emission spectroscopy (OES) of these plasmas reveal that NH* species are formed in the DBD and MW ammonia-containing plasmas (51). Meanwhile, N_2* and N_2^+ species form preferentially in the DBD and MW nitrogen plasmas, respectively. We can therefore conclude that NH* species are more efficient than other nitrogen species for the nitrogen functionalization of PET. We reached a similar conclusion for plasma treated DLC (diamond like carbon) (51). In addition, the derivatization experiments (see Table 1) indicate that ammonia containing plasmas favor the incorporation of amine groups onto the surface of PET. Previous OES analysis of the MW and DBD plasmas used in the present work also showed that small peaks due to O* and OH* species are detected in the DBD/Ar + NH_3 plasma (51). It is likely that these species, even if not always detected, also form under the working conditions of the present experiment. Thus, the increase in oxygen surface concentration on the plasma-treated PET seems to be related with the presence of these impurity species whose formation is practically unavoidable in most practical plasma reactors. In the next section, we will discuss how these oxygen functional groups are critical to increase the hydrophilic character of the surface.

Hydrophilic Character of Amine Groups and Aging Effects. WCA can be affected by both the roughness of the surfaces and their chemistry. The influence of the first parameter can be rationalized by, for example, the classical models of Wenzel (59) or Cassie (60) when the roughness is in the order of the micrometer. Thus, even if a change in roughness is found after the plasma treatment of PET, particularly for the DBD plasmas (see Table 2), its magnitude is not as high as to expect a significant influence onto the WCAs. We must therefore admit that the surface roughness does not play a significant role in controlling the wetting properties and that the new surface groups are the main cause of the hydrophilicity of the plasma-treated samples. Our investigation also suggests that the WCA variations in PET-treated with nitrogen plasmas are mainly due to the incorporation of oxygen functional groups onto its surface and that nitrogen groups are rather inactive in producing such an effect. In fact, for PET treated with the beam of neutral species, the very small decrease in WCA and the practically constant value of the surface tension suggest that nitrogen surface groups, the only ones effectively formed by these treatments, do not contribute significantly to the changes in the polar component of surface tension. This suggests that WCA in nitrogen plasma treated polymers and the hydrophilic character of their surfaces are mainly due to the presence of oxygen groups incorporated during the plasma treatment and that nitrogen functional groups, including amine groups, do not present a significant hydrophilic character as previously claimed in literature (20, 23). In this regard, it must be mentioned that previous studies in literature have shown that amine groups formed on polyethylene are more stable when kept for a long time in a phosphate buffer solution than in air (26), a result that sustains that no significant change in amine concentration has occurred during the analysis of the WCA of our samples by the sessile method.

Another significant effect of aging refers to the decrease of nitrogen concentration from the topmost surface layers (c.f., Table 1). This phenomenon may be produced by either the rearrangement of the polymer chains as claimed above for the oxygen surface groups, the surface reaction with chemical agents in the atmosphere (e.g., water, oxygen, etc.), or both. The formation of amides by reaction with agents from the atmosphere has been claimed as a very effective process for amine containing polymers exposed to air (25). In particular, our results in Figure 4 show that aging leads to a substantial decrease in the concentration of amine groups at the surface, although at the present stage we cannot conclude about the relative importance of the removal mechanisms. The only clue clearly evidenced by our experimental results is the fact that the amine removal is complete for PET treated with the plasmas of N_2 and the beam of nitrogen species. Because this removal is only partial on surfaces functionalized with ammonia, it is reasonable to assume that the excess of hydrogen, likely incorporated in PET during the ammonia treatment, must contribute to stabilize the amine groups on the surface and/or to prevent their migration to the bulk or their reaction with the atmosphere.

Depth Distribution Profiles in Plasma-Treated PET. The XPS background analysis of the treated PET has shed some light onto the effects of plasma and beam treatments on the composition of its upmost layers (i.e., up to about 6 nm) and its evolution with aging. The depth profiles analysis reported in Figure 6, confirmed by the angle-resolved analysis of the same samples, provide a close look to the oxygen and carbon distributions through the most external layers of PET. The quite different depth profiles determined for the plasma- and beam-treated surfaces further support that impurity oxygen species in the plasmas are responsible for the increase in the oxygen content at the topmost layers of the plasma treated PET. Thus, the experiments with the beams of neutral species, where the presence of oxygen species can be discarded, show no significant enrichment of oxygen at the topmost surface layers (in the case of the treatment with the nitrogen beam, oxygen is even depleted from the topmost surface layers as evidenced by the corresponding depth profile in Figure 6). On the other hand, the analysis of the depth profiles of the aged samples is in all cases congruent with a recovery of the original state of the surface 1 month after

the treatments. The tendency is always toward restoring the original flat distribution of oxygen and occurs independently on whether the initial situation presented enrichment or depletion of oxygen in the two/three topmost nanometers of the sample. Very likely, the rearrangement of the polymer chains, a phenomenon generally admitted as the cause of this type of changes in the concentration of functional groups at the outmost surface layer in plasma treated polymers (20), is responsible for this finding. It is important to note that with the background analysis method proposed here, we have proved that the changes induced by the plasma/beam treatments affect not only the topmost surface layer but a thickness of several nanometers.

5. CONCLUSIONS

The previous results and discussion have shown that nitrogen plasma activation of PET can be very effective at incorporating nitrogen surface groups onto its surface. It is found that Ar + NH_3 plasmas, particularly based on DBD processes, are the most efficient for this purpose. However, surface functionalization of PET in conventional low-pressure or atmospheric plasma reactors produces not only the incorporation of nitrogen surface groups but also an enrichment of oxygen at the topmost surface layers (2−3 nm) of the treated polymers. Incorporation of nitrogen functional groups without increasing the overall concentration of oxygen in the surface is possible under very strict vacuum conditions using a source of neutral species (i.e., N and N−H_x). In this case, a depletion of oxygen can even occur at the 2−3 topmost surface layer of the polymer. Background shape analysis has revealed as a very powerful tool to account for this type of changes in plasma and beam treated PET.

From a practical point of view, it is also important to stress that our results with the beam-treated samples suggest that nitrogen functional groups (among other −NH_2, determined by derivatization) practically do not affect the surface tension of functionalized polymers. The previous attribution of changes in this magnitude to the presence of nitrogen species (21) is therefore not supported by our results and could contribute to flaw assessments of the surface reactivity of plasma treated polymers. It is also important to note that the concentration of amine groups on the surface is in general higher after the treatments with ammonia and that these groups persist for longer periods of time on these surfaces.

Acknowledgment. We thank the Ministry of Science and Education of Spain (Projects MAT 2007-65764/NAN2004-09317, and the CONSOLIDER INGENIO 2010-CSD2008-00023) and the Junta de Andalucía (Projects TEP2275 and P07-FQM-03298) for financial support.

Supporting Information Available: Evolution of the atomic concentration on PET subjected to treatments with the N and NH_x beams for increasing periods of time, percentage of oxygen as a function of the takeoff angle determined by XPS on the surface of PET subjected to treatment with a MW/Ar+NH_3 plasma and with the beam of NH_x species, and Cl2p spectra detected by XPS analysis after derivatization on the nitrogen plasma-treated surfaces of PET (PDF). This material is available free of charge via the Internet at http://pubs.acs.org.

REFERENCES AND NOTES

(1) Noeske, M.; Degenhardt, J.; Strudthoff, S.; Lommatzch, U. *Int. J. Adhes. Adhes.* **2004**, *24*, 171–177.
(2) Kotal, V.; Svorcik, V.; Slepicka, P.; Sajdl, P.; Blahova, O.; Sutta, P.; Hnatowicz, V. *Plasma Process. Polym.* **2007**, *4*, 69–76.
(3) Mercx, F. P. M. *Polymer* **1994**, *35* (10), 2098–2107.
(4) Oehr, C.; Müller, M.; Elkin, B.; Hegemann, D.; Vohrer, U. *Surf. Coat. Technol.* **1999**, *25*, 116–119.
(5) Chu, L.; Knoll, W.; Förch, R. *Plasma Process. Polym.* **2006**, *3*, 498–505.
(6) Tajima, S.; Komvopoulos, K. *Appl. Phys. Lett.* **2006**, *89*, 124102.
(7) Grace, J. M.; Gerenser, L. J. *J. Dispersion Sci. Technol.* **2003**, *24*, 305–341.
(8) Gerenser, L. J.; Grace, J. M.; Apai, G.; Thompson, P. M. *Surf. Interface Anal.* **2000**, *29*, 12–22.
(9) Badey, J. P.; Espuche, E.; Sage, D.; Chabert, B.; Jugnet, Y.; Batier, C.; Duc, T. M. *Polymer* **1996**, *37* (8), 1377–1386.
(10) Narushima, K.; Yamashita, N.; Fukuoka, M.; Inagaki, N.; Isono, Y.; Islam, M. R. *Jpn. J. Appl. Phys.* **2007**, *46*, 4238–4245.
(11) Borcia, G.; Chipre, A.; Rusu, I. *Plasma Sources Sci. Technol.* **2006**, *15*, 849–857.
(12) Dai, C.-A.; Lee, Y.-H.; Chiu, A.-C.; Tai-An, T.; Keng-Jen, L.; Kai-Ling, C.; Ming-Wei, L. *Polymer* **2006**, *47*, 8583–8594.
(13) Truica-Marasescu, F.; Wertheimer, M. R. *Plasma Process. Polym.* **2008**, *5*, 44–57.
(14) Kang, E. T.; Neoh, K. G.; Li, Z. F.; Tan, K. L.; Liaw, D. J. *Polymer* **1998**, *39* (12), 2429–2436.
(15) Shard, A. G.; Whittle, J. D.; Beck, A. J.; Brookes, P. N.; Bullet, N. A.; Talib, R. A.; Mistry, A.; Barton, D.; McArthur, S. L. *J. Phys. Chem. B* **2004**, *108*, 12472–12480.
(16) Arefi-Khonsari, F.; Tatoulian, M.; Bretagnol, F.; Bouloussa, O.; Rondelez, F. *Surf. Coat. Technol.* **2005**, *200*, 14–20.
(17) Bullet, N. A.; Bullet, D. P.; Truica-Marasescu, F.-E.; Lerouge, S.; Mwale, F.; Wertheimer, M. R. *Appl. Surf. Sci.* **2004**, *235*, 395–405.
(18) Meyer-Plath, A. A.; Schröder, K.; Finke, B.; Ohl, A. *Vaccum* **2003**, *71*, 391–406.
(19) Meyer-Plath, A. A.; Finke, B.; Schröder, K.; Ohl, A. *Surf. Coat. Technol.* **2003**, *174/175*, 877–881.
(20) Vesel, A.; Junkar, I.; Cvelbar, U.; Kovac, J.; Mozetic, M. *Surf. Interface Anal.* **2008M**, *40*, 1444–1453.
(21) Narushima, K.; Yamashita, N.; Isono, Y.; Islam, M. R.; Takeuchi, M. *Jpn. J. Appl. Phys.* **2008**, *47* (5), 3603–3605.
(22) Inagaki, N.; Narushim, K.; Tuchida, N.; Miyazaki, K. *J. Polym. Sci., Part B: Polym. Phys.* **2004**, *42*, 3727–3740.
(23) Morent, R.; De Geyter, N.; Gengembre, L.; Leys, C.; Payen, E.; Van Vlierberghe, S.; Schacht, E. *Eur. Phys. J. Appl. Phys.* **2008**, *43*, 289–294.
(24) Li, R.; Chen, J. *Plasma Sci. Technol.* **2006**, *8* (3), 325–328.
(25) Gengenbach, T. R.; Griesser, H. J. *J. Polym. Sci., Part A: Polym. Chem.* **1999**, *37*, 2191–2206.
(26) Ghasemi, M.; Minier, M.; Tatoulian, M.; Arefi-Khonsari, F. *Langmuir* **2007**, *23*, 11554–11561.
(27) Massines, F.; Gouda, G. *J. Phys. D: Appl. Phys.* **1998**, *31*, 3411–3420.
(28) Fridman, A.; Chirokov, A.; Gutsol, A. *J. Phys. D: Appl. Phys.* **2005**, *38*, R1–R24.
(29) van Oss, C. J. *Interfacial Forces in Aqueous Media*; Marcel Decker: New York, 1994.
(30) Jańczuk, B.; Kerkeb, M. L.; Bialopiotrowicz, T.; González- Caballero, F. *J. Colloid Interface Sci.* **1992**, *151*, 333–342.
(31) Tougaard, S. *J. Vac. Sci. Technol.* **1996**, *A 14*, 1415–1423.
(32) Tougaard, S. *Surf. Interface Anal.* **1998**, *26*, 249–269.
(33) López-Santos, C.; Yubero, F.; Cotrino, J.; Barranco, A.; González-Elipe, A. R. *J. Phys. D: Appl. Phys.* **2008**, *41*, 225209–225221.
(34) Markkula, T. K.; Hunt, J. A.; Pu, F. R.; Williams, R. L. *Surf. Interface Anal.* **2002**, *34*, 583–587.
(35) Favia, P.; Stendardo, M. V.; d'Agostino, R. *Plasmas Polym.* **1996**, *1*, 91–112.
(36) Chevallier, P.; Castonguay, M.; Turgeon, S.; Dubrulle, N.; Mantovani, D.; McBreen, P. H.; Wittmann, J.-C.; Laroche, G. *J. Phys. Chem. B* **2001**, *105* (50), 12490–12497.

(37) Moisan, M.; Zakrzewski, Z.; Pantel, R. *J. Phys. D: App. Phys.* **1979**, *12*, 219–237.
(38) Moisan, M.; Zakrzewski, Z. *J. Phys. D: Appl. Phys.* **1991**, *24*, 1025–1048.
(39) Lebedev, Y. A.; Epstein, I. L.; Tatarinov, A. V.; Shakhatov, V. A. *J. Phys.: Confe. Ser.* **2006**, *44*, 30–39.
(40) Kim, J. H.; Choi, Y. H.; Hwang, Y. S. *Phys. Plasma* **2006**, *13*, 093501–093507.
(41) Li, H.; Xu, T.; Wang, C.; Chen, J.; Zhou, H.; Liu, H. *Diamond Relat. Mater.* **2006**, *15*, 1585–1592.
(42) Endrino, J. L.; Marco, J. F.; Allen, M.; Poolcharuansin, P.; Phani, A. R.; Albella, J. M.; Anders, A. *Appl. Surf. Sci.* **2008**, *254*, 5323–5328.
(43) Riedo, E.; Comin, F.; Chevrier, J.; Schmithusen, F.; Decossas, S.; Sancrotti, M. *Surf. Coat. Technol.* **2000**, *125*, 124–128.
(44) Choukourov, A.; Biederman, H.; Kholodkov, I.; Slavinska, D.; Trchova, M.; Hollander, A. *J. Appl. Polym. Sci.* **2004**, *92*, 979–990.
(45) Tougaard, S. *QUASES, Software Package for Quantitative XPS/AES of Surface Nanostructures by Inelastic Peak Shape Analysis*; see www.QUASES.com
(46) Strobel, M.; Jones, V.; Lyons, Ch. S.; Ulsh, M.; Kushner, M. J.; Dorai, R.; Branch, M. *Plasmas Polym.* **2008**, *8*, 61–95.
(47) Owens, D. K.; Wendt, R. C. *J. Appl. Polym. Sci.* **1969**, *13*, 1741–1747.
(48) Ramires, P. A.; Mirenghi, L.; Romano, A. R.; Palumbo, F.; Nicolardi, G. *J. Biomed. Mater. Res.* **2000**, *51*, 535–539.
(49) Le, Q. T.; Pireaux, J. J.; Verbist, J. *J. Surf. Interface Anal.* **1994**, *22*, 224–229.
(50) Gonzalez, II E.; Barankin, M. D.; Guschl, P. C.; Hicks, R. F. *Langmuir* **2008**, *24*, 12636–12643.
(51) Lopez-Santos, C.; Cotrino, J.; Yubero, F.; Contreras, L.; Barranco, A.; González-Elipe, A. R. *Plasma Process. Polym.* **2009**, *6*, 555–565.
(52) Kull, K. R.; Steen, M. L.; Fisher, E. R. *J. Membr. Sci.* **2005**, *246*, 203–215.
(53) Finke, B.; Schröder, K.; Ohl, A. *Plasma Process. Polym.* **2008**, *5*, 386–396.
(54) Tanuma, S.; Powell, C. J.; Penn, D. R. *Surf. Interface Anal.* **1993**, *21*, 165–176.
(55) Junkar, I.; Cvelbar, U.; Vesel, A.; Mozetic, M. *Plasma Process. Polym.* **2009**, *6*, 667–675.
(56) Bhoj, A. N.; Kushner, M. J. *J. Phys. D: Appl. Phys.* **2007**, *40*, 6953–6968.
(57) Bhoj, A. N.; Kushner, M. J. *J. Phys. D: Appl. Phys.* **2006**, *39*, 1594–1598.
(58) Bhoj, A. N.; Kushner, M. J. *Plasma Sources Sci. Technol.* **2008**, *17*, 035025—035040.
(59) Wenzel, R. N. *Ind. Eng. Chem.* **1936**, *28*, 988–994.
(60) Cassie, A. B. D.; Baxter, S. *Trans. Faraday Soc.* **1944**, *40*, 546–551.

AM100052W